CARBON 47 (2009) 102–108

available at www.sciencedirect.com

ScienceDirect

journal homepage: www.elsevier.com/locate/carbon

Polymer electrolyte fuel cells employing electrodes with gas-diffusion layers of mesoporous carbon derived from a sol–gel route

A.K. Sahu[a], K.G. Nishanth[a], G. Selvarani[a], P. Sridhar[a], S. Pitchumani[a], A.K. Shukla[a,b,*]

[a]Central Electro-Chemical Research Institute, Karaikudi 630 006, India
[b]Solid State and Structural Chemistry Unit, Indian Institute of Science, Bangalore 560 012, India

ARTICLE INFO

Article history:
Received 20 May 2008
Accepted 10 September 2008
Available online 18 September 2008

ABSTRACT

Sol–gel derived mesoporous carbon (MC) for the preparation of gas-diffusion layer (GDL) and its ameliorating effect on the performance of polymer electrolyte fuel cells (PEFCs) is reported. MC with a specific surface area of 370 m^2/g, pore diameter of 6.7 nm and pore volume of 0.45 cm^3/g has been synthesized by co-assembly of a tri-block copolymer, namely pluronic-F127, as a structure directing agent, and a mixture of phloroglucinol and formaldehyde as carbon precursor. X-ray diffraction and transmission electron microscopy have been employed to examine the structural properties of the MC. Surface morphology of the GDL comprising MC has been studied by scanning electron microscopy. A peak power density of 0.53 W/cm^2 at a load current-density of 1.1 A/cm^2 is achieved for the PEFC employing electrodes with GDL of MC compared to the peak power density of 0.47 W/cm^2 at a load current-density of 0.93 A/cm^2 for the PEFC employing electrodes with GDL of commercial Vulcan XC-72R carbon, while operating at 70 °C with H_2 and air feeds at atmospheric pressure.

1. Introduction

Being energy efficient and environmentally benign, fuel cells are emerging as the energy-conversion machines for portable, mobile and stationary power applications [1]. Among various types of fuel cells, polymer electrolyte fuel cells (PEFCs) are most attractive due to their quick start-up capability under ambient conditions. In recent years, although ground-breaking progress has been made in terms of membranes, anodic/cathodic catalysts, bipolar-plate materials as well as the system design, a major performance limiting-factor for PEFCs remains to be the lack of optimal distribution of reactant gases within the solid–liquid–gas (SLG) interface of the electrodes. At the SLG interface, solid phase exists as high surface area carbon, liquid phase as water and gas phase as reactant gas. The distribution of micropores (<2 nm) and mesopores (2–50 nm) in the carbon is central to the optimal distribution of liquid water and reactant gas at the SLG interface. PEFC electrodes generally comprise a backing layer, a gas-diffusion layer (GDL) and a catalyst layer. Among these, it is the GDL that primarily dictates the distribution of the reactant gas at the SLG interface. The GDL comprises a hydrophobic substance dispersed in hydrophilic carbon wherein the porous nature of the latter plays a seminal role on the performance of the PEFC. The multi-faceted functionality of the GDL includes reactant-gas distribution, water transport, electron transport, heat conduction and mechanical support to the membrane electrode assembly. In addition to various aforesaid physical parameters of the GDL, gas permeability and pore size distribution also determine the limiting load current-density of the fuel cell, especially when air is used on the oxidant side [2].

The most widely used materials for GDL are Vulcan XC-72R, pearl black, acetylene black and Ketjen black. Jordan

* *Corresponding author:* Address: Central Electro-Chemical Research Institute, Karaikudi 630 006, India. Fax: +91 4565 227779.
E-mail address: shukla@sscu.iisc.ernet.in (A.K. Shukla).
0008-6223/$ - see front matter
doi:10.1016/j.carbon.2008.09.031

et al. [3] have shown that acetylene black, with a low pore volume and an optimized thickness, gave a better performance in PEFCs than Vulcan XC-72R carbon. Neergat et al. [4] have reported that Ketjen black carbon with a high surface area gave better performance than acetylene black or Vulcan XC-72R in a direct methanol fuel cell. It could be argued that the dominant microporous structure of the above cited activated carbon materials could restrict the optimal distribution of reactant at the SLG interface of the electrode. To address this issue, efforts have been expended to develop new carbon nano-materials with higher surface area and/or higher electrical conductivity than activated carbon materials and their feasibility explored for fuel cell electrodes. Graphitic carbon frameworks include carbon nanotubes, carbon nanofibers, carbon nanohorns, carbon nanocages and graphitic porous carbon, which have been the subject of continuing research and development [5–9]. Kannan et al. [10] studied the application of single-walled carbon nanotubes (SWCNTs), pearl black (PB) and their combination as GDL and their effect on the performance of PEFCs. A combination of SWCNT and PB gives higher performance for PEFC as compared to pristine SWCNT and PB, mainly due to a better distribution of the reactant gases at the SLG interface. Ironically, harsh synthetic conditions and low production yields limit large-scale and cost-effective production of SWCNTs. Mesoporous carbon (MC) materials, comprising regular arrays of uniform mesopores, are highly attractive from the viewpoint of pore structure and pore sizes (2–50 nm) that provide improved mass transport, electron transport and easy removal of product water from the fuel cell [11–13].

Over the last decade, there has been considerable interest in the synthesis and development of MC as these possess attractive textural and structural features like, highly ordered-structures, high surface areas, and wide pore range and pore size distribution. Ordered mesoporous carbon (OMC) materials with tunable pore sizes and pore structures can be prepared from hard template methods that include: (i) forming a composite by filling the nano-channels of hard template (usually SBA-15, MCM-48 and colloidal silica) with appropriate carbon precursors, (ii) carbonization of the composite at high temperature, and (iii) removal of templates with aqueous NaOH or HF [14,15]. Accordingly, the fabricated porous carbons happen to be the structural replica of the hard template. In this process, an additional step is mandatory to prepare silica templates prior to the multistep template synthesis making it a long and complicated process [16]. Therefore efforts have also been made to synthesize OMC materials without the hard template route [17]. Although, these classes of MCs show some irregularly interconnected pores and relatively wider distribution of pore sizes than OMCs, their synthesis is simple and mesoporous structures can be controlled by varying the molar ratio of the respective precursors. For example, ordered hexagonal MC films have been prepared through the direct carbonization of a thermosetting polymeric carbon precursor and a thermally decomposable surfactant [18–21]. Zhao et al. [22,23] synthesized OMC powder through direct assembly of a tri-block copolymer (P123) and resol. Subsequently, OMC materials with varying structures, namely hexagonal, cubic and lamellar frameworks, were synthesized by simply adjusting the molar ratio of the polymer precursors and amphiphilic surfactants [23]. Aerosol-assisted methods have also been reported for the synthesis of MCs [24].

This study demonstrates the ameliorated performance of the PEFC electrodes with GDL of a sol–gel derived MC. The study includes the synthesis of OMC structures based on commercially available tri-block copolymer (pluronic F127, $EO_{106}PO_{70}EO_{106}$) as a structure directing agent and a mixture of phloroglucinol and formaldehyde as a cost-effective carbon precursor by a sol–gel route. The resultant high surface area MC is used as GDL and its effect on the performance on PEFC is studied. The mesoporous GDL with favorable surface area and pore size distribution (PSD) helps ameliorating the liquid water flux through the GDL with minimum flooding and improves oxygen diffusion to the catalyst layer during the fuel cell operation.

2. Experimental

2.1. Materials

Phloroglucinol dihydrate (99%, Acros Organics), pluronic F127 (Sigma–Aldrich, Inc.), formaldehyde (37–41%) and absolute ethanol (both obtained from Merck, Germany), hydrochloric acid (HCl) (37%, sd-fine chemicals, India) were used as received. De-ionized water (18.4 MΩ cm) used for experiments was produced by a Millipore system.

2.2. Synthesis of MC

A soft-template route described elsewhere [20] was adopted for the preparation of MC. In brief, 1.25 g phloroglucinol and 1.25 g pluronic F127 were dissolved into 9 g of 10:9 wt. ratio of ethanol and water mixture. Subsequently, the solids were dissolved under magnetic stirring at room temperature; 0.1 g of HCl was added to the solution as a catalyst. The solution was stirred at room temperature for additional 30 min till a light pink color appeared. Following this, 1.3 g of formaldehyde was added to the above solution. The solution turned cloudy after 30 min and separated into two layers after 1 h. The upper layer mainly consisted of the mixture of water and ethanol, while the lower layer was a clear polymer-rich solution. The polymer solution was kept on continued stirring overnight to form an elastic but non-sticky monolith that was further cured at 100° C overnight. The materials were then carbonized in a tubular furnace under nitrogen atmosphere via heating ramps of 1 °C/min from 100 to 400 °C, 5 °C/min from 400 to 850 °C and then kept at 850 C for 2 h. In order to maintain the high surface area of MC, the carbonization temperature in this study was limited to 850 °C. The sample was allowed to cool to the room temperature. The materials were collected and ground to fine powders. MC was treated by refluxing in HNO_3 (1, 2 and 3 M) at boiling conditions for 2 h in each case in order to create oxygen surface groups. After oxidation, samples were recovered and washed copiously with de-ionized water until the pH was close to 7 followed by overnight drying at 90 °C.

2.3. Physical and structural characterization

For the structural characterization, X-ray diffraction (XRD), scanning electron microscopy (SEM) and transmission electronic microscopy (TEM) were used. XRD patterns at small angles ($2\theta = 0.2–5^{o}$) were recorded using a BRUKER NANOSTAR SAXS system with a θ–θ configuration and using CuK_{α} radiation. The surface morphology of the carbon particles coated over a macroporous substrate was observed with the help a JEOL JSM 5400 SEM. TEM images for determination of pore size and their distribution were obtained using a 200 KV Tecnai-20 G2. For these measurements, the samples were suspended in acetone with ultrasonic dispersion for 3 min. Subsequently, a drop of this suspension was deposited on a holey carbon grid and allowed for drying. TEM images of the samples were recorded both in the axial direction of the ordered hexagonal pores as also in the perpendicular direction. Images were recorded with a MultiScan CCD camera (model 794, Gatan) using low-dose conditions. Textural and surface properties of carbon supports were characterized by N_2-physisorption and temperature programmed desorption, respectively. Nitrogen adsorption–desorption isotherms were measured at 77 K using a Micromeritics ASAP 2020. Total surface area and pore volumes were determined using the Brunauer–Emmett–Teller (BET) equation and the single point method, respectively. PSD curves were obtained by Barrett–Joyner–Halenda (BJH) method and the position of the maximum of the PSD was used as the average pore diameter. The point-of-zero-charge (PZC) measurements were carried out for both MC and MC treated with 2 M HNO_3 with pH adjusted de-ionized water. The pH was adjusted using different normality values of HCl and NaOH. The PZC was measured using a pH meter (Elico-127L) adopting the procedure described elsewhere [25]. Before measuring PZC, both the modified and pristine MCs were washed copiously with hot de-ionized water followed by drying in an air oven at 80 °C. The pH of adjusted de-ionized water was taken as the initial pH. Finally, the calculated amounts of MC and MC treated with 2 M HNO_3 were separately added to sample bottles containing de-ionized water at different pH values followed by sonication for 1 h. The pH was measured and recorded as the final pH. Air permeability of GDLs comprising Vulcan XC-72R, MC and MC treated with 2 M HNO_3 were also measured with Automated Capillary Flow Porometer: CFP-1500-AEXBB, Porous Materials, Inc., US. The working diameter (1 cm) and the thickness (0.4 mm) were kept identical for all samples. The tests were performed with differential air-pressure applied to the samples and the corresponding air flow rates through the porous GDLs were recorded.

2.4. Fuel cell performance

Performance of the PEFCs comprising MC and treated MC as GDL were examined both in H_2/O_2 and H_2/air modes and the results were compared with the PEFC comprising Vulcan XC-72R as GDL. For making membrane electrode assemblies (MEAs), Toray carbon papers of thickness 0.37 mm with 15 wt.% teflonization were used both for anode and cathode. For the diffusion layers, carbon slurry was prepared by dispersion of synthesized MC in 2-propanol with 15 wt.% poly-tetrafluoro ethylene (PTFE) under ultra sonication. The resultant slurry was applied onto the macro porous support with a loading of 1.5 mg/cm^2 on both the electrodes followed by sintering in a muffle furnace at 350 °C for 30 min. For the catalyst layer, 40 wt.% Pt/C (Johnson Matthey) was dispersed in a mixture of 2-propanol and Nafion solution followed by ultrasonication for 20 min to form a homogeneous slurry. The slurry was then applied to the diffusion layer. The catalyst loading on both the anode and the cathode (active area = 25 cm^2) were kept at 0.5 mg/cm^2. A thin layer of Nafion ionomer was applied to catalyst surface of both the electrodes. MEAs were obtained by hot pressing the Nafion-1135 membrane sandwiched between cathode and anode under 15 kN (~60 kg/cm^2) at 125 °C for 3 min. The MEAs were evaluated using a conventional 25 cm^2 fuel cell fixture with parallel serpentine flow field machined on graphite plates (Schunk Kohlenstofftechnic). The cells were tested at 70 °C with gaseous hydrogen and gaseous oxygen/air fed at atmospheric pressure at the anode and cathode sides, respectively. The flow rates for both hydrogen and oxygen/air gases were kept at 1 L/min using mass flow controllers (Aalborg Instruments and Controls, US). Both the gaseous reactants were passed through humidifiers before feeding them to the cell. After establishing the desired experimental conditions (dew point temperature 80 °C, gas temperature/gas supply temperature 85 °C, and dew point humidification temperature 85 °C)

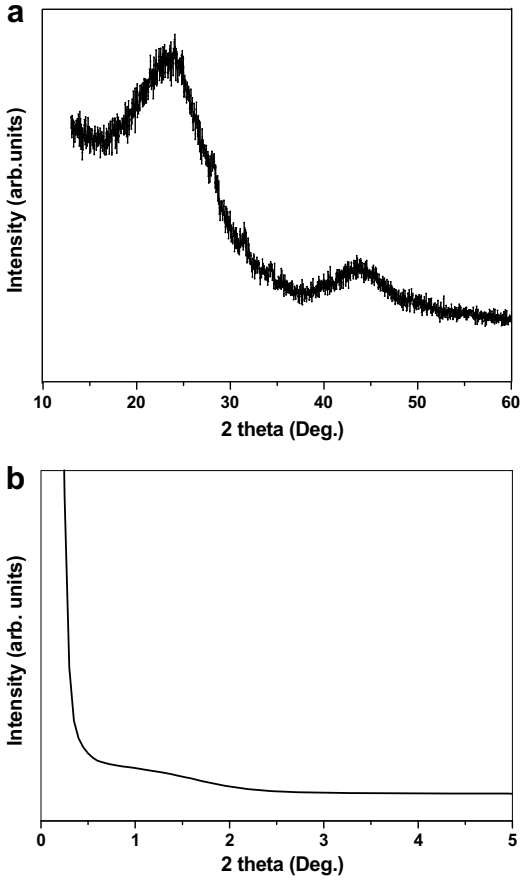

Fig. 1 – (a) Powder XRD pattern for MC and (b) low-angle XRD pattern for MC.

galvanostatic polarization data were obtained under steady-state condition on the PEFCs using a fuel cell test station (model PEM-FCTS-158541) supplied by Arbin Instruments, US. The reproducibility of the data was ascertained by repeating the experiments at least twice.

3. Results and discussion

Powder XRD pattern for the synthesized MC shown in Fig. 1a exhibits characteristic XRD peaks at 23° and 43° confirming the carbonaceous nature of the sample with low crystallinity. Fig. 1b shows the typical small-angle XRD pattern of as prepared MC with a peak at small angles indicating the presence of mesoporous structure as observed by Liang et al. [20].

Fig. 2a and b shows the N_2 sorption isotherms of as prepared MC and MC treated with 2 M HNO_3 and their corresponding PSDs. Both MCs show type IV isotherm with pronounced hysteresis loop with a sharp capillary condensation at a high relative pressure, indicating the presence of relatively large pores, while type II isotherm is typically observed for non-porous or macro-porous materials. The respective BET surface areas of as prepared MC and MC treated with 2 M HNO_3 are found to be 370 and 354 m^2/g, respectively. The PSD analysis derived from the adsorption branch of the isotherms indicates two populations of mesopores at 3.9 and 7.6 nm for as-prepared MC. Similarly, the PSD for MC treated with 2 M HNO_3 shows two populations of mesopores at 3.84 and 6.4 nm. In brief, the average BJH pore diameters of the as-prepared MC and MC treated with 2 M HNO_3 are

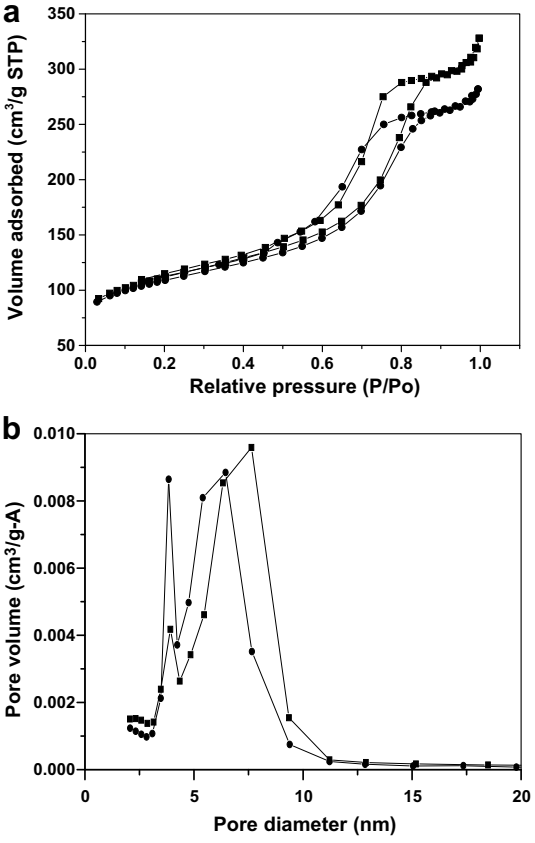

Fig. 2 – (a) N_2 sorption isotherm for (■) as prepared MC and (●) MC treated with 2 M HNO_3 and (b) corresponding PSD for (■) as prepared MC and (●) MC treated with 2 M HNO_3.

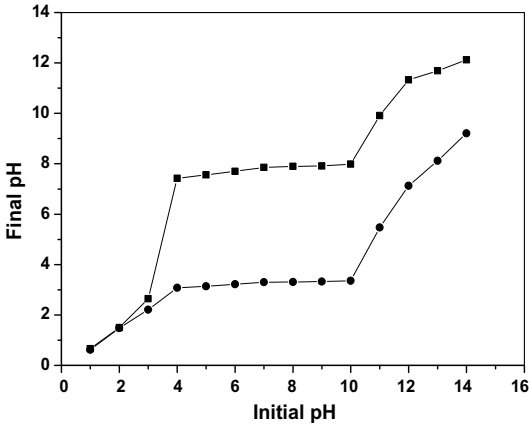

Fig. 3 – PZC for (■) as prepared MC and (●) MC treated with 2 M HNO_3.

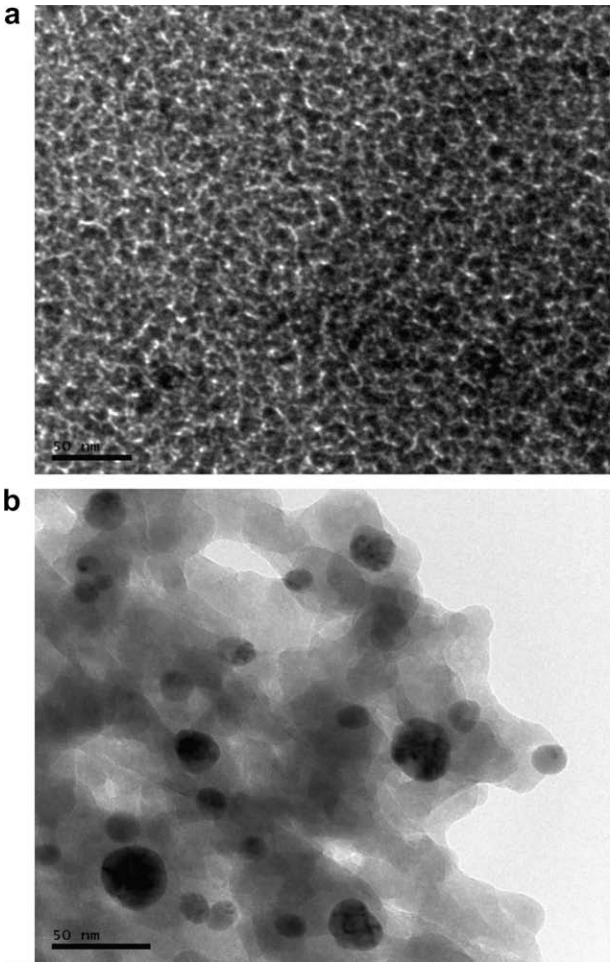

Fig. 4 – (a) TEM pictures for as synthesized MC and (b) MC treated with 2 M HNO_3. The scale bar in both the pictures is 50 nm.

6.74 and 5.92 nm, respectively. The pore volumes for as-prepared MC and MC treated with 2 M HNO_3 calculated from the adsorption isotherm are 0.45 and 0.38 cm^3/g, respectively. Reduction in surface area, pore diameter and PSD for treated MC is due to the partial distortion of the mesoporous nature of the carbon. In relation to the activated carbons like Vulcan XC-72R that has a BET surface area of 235 m^2/g with microporous nature (<2 nm) [26,27], MC has high surface area with large pore sizes and pore volumes. It is noteworthy that the graphitic carbon synthesized by pyrolysis of ethanol with dissolved iron carbonyl prepared at 600, 700 and 900 °C had BET surface areas of 800, 433 and 201 m^2/g, respectively [8]. In the present study, MC synthesized at 850 °C exhibits a surface area of 370 m^2/g in agreement with the literature [8].

For an estimation of oxygen-containing surface groups in MC treated with nitric acid, the PZC measurements are carried out with the final pH as a measure of the strong buffering effect. The initial pH versus final pH for MC and MC treated with 2 M HNO_3 are depicted in Fig. 3. The PZC is obtained from the horizontal part of the curve for different types of MC. The PZC values for the MC and MC treated with 2 M HNO_3 are 7.7 and 3.2, respectively. From the data, it is clearly reflected that nitric acid treatment of the MC introduces acidic groups, like −COOH, that contain active oxygen surface and bring down the PZC. A larger reduction in PZC value for the MC treated with HNO_3 in relation to the pristine MC strongly influences the charge density on the MC to which the acidic groups is attached.

TEM study further corroborates these observations. Fig. 4a shows the TEM picture for as-prepared MC and Fig. 4b shows the TEM picture for the treated MC. In the case of as-prepared MC, no long-range pore ordering is observed but instead a worm-like structure is clearly revealed. It is noteworthy that the absence of long-range pore ordering is obtained without usage of any hard-template approach during synthesis of MC but by mere use of pluronic-F127 as a mild structure directing agent. The pores typically have a diameter of ~7 nm in accordance with the results obtained from the nitrogen-sorption study. After oxidation treatment, the structure is maintained with partial distortion in its pores.

Fig. 5a–c shows SEM micrographs of GDL layers utilizing Vulcan XC-72R, as prepared MC and MC treated with 2 M HNO_3, respectively. The GDL coated with Vulcan XC-72R shows homogeneous carbon distribution with surface cracks. By contrast, GDL of MC shows uniform carbon distribution and crack-free surface which facilitates the reactant gas to diffuse to the active catalyst sites. The GDL layer with treated carbon also shows an almost similar surface morphology indicating that after nitric acid treatment of the MCs the surface characteristics are retained.

The GDLs comprising different carbons are also evaluated for their air permeability prior to their use in the fuel cell. Fig. 6 shows the air flow rate versus differential air-pressure for different GDLs. The data suggest the air flow rate for all the samples to increase with pressure. The MC treated with HNO_3 is a little lower in air permeability in relation to the pristine MC. This may be due to the decrease in the pore size of treated carbon (Fig. 2). In general, the GDL coated with MC shows higher gas permeability in relation to the GDL coated with Vulcan XC-72R. The high gas-permeability of the GDL comprising MC is a desired feature in fuel cell operation.

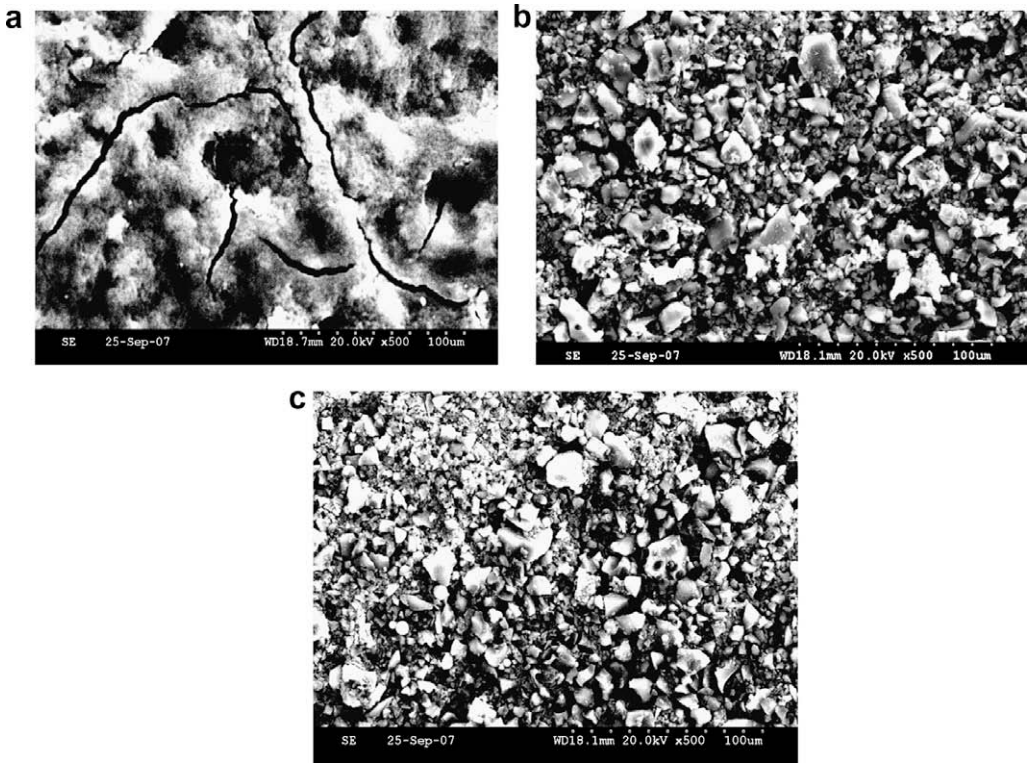

Fig. 5 – (a) SEM images for GDL layers comprising Vulcan XC-72R, (b) as prepared MC, and (C) MC treated with 2 M HNO_3.

The performance of PEFC gas-diffusion electrodes employing Vulcan XC-72R, MC and treated MC are studied from the polarization data. In this study, we have investigated the effect of oxidation environment at which high amount of surface groups can be created, while maintaining the structural order of MC. To ascertain this, various MEAs with different treated carbon have been realized and studied to quantify their effect on the fuel cell performance. This has enabled to identify the ideal mesoporous structure and the optimal functionalization level. Fig. 7 compares the polarization curves at 70 °C for all MEAs under fully-wet condition (100% relative humidity) with gaseous-reactants fed at atmospheric pressure. The PEFC with GDL of Vulcan XC-72R shows a peak power density of 0.74 W/cm^2 at a load current-density of 1.65 A/cm^2. By contrast, the GDL with non-treated MC delivers 0.69 W/cm^2 at a load current-density of 1.5 A/cm^2, which is a little lower in power density in relation to commercial Vulcan XC-72R. Interestingly, an increase in power density value is observed with the GDL coated with treated MC. A maximum power density of 0.79 W/cm^2 at a load current-density of 1.65 A/cm^2 is observed with the GDL of MC treated with 2 M HNO_3.

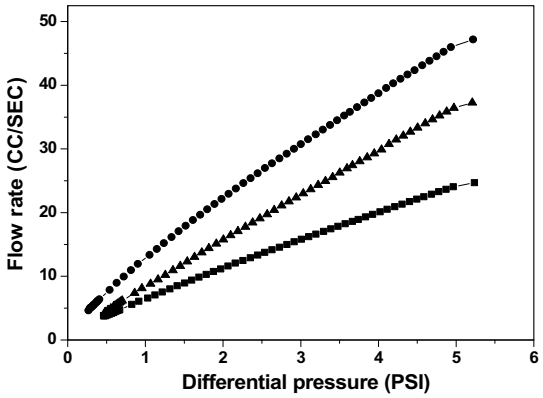

Fig. 6 – Gas permeability for the GDL of (■) Vulcan XC-72R, (●) as prepared MC and (▲) MC treated with 2 M HNO_3.

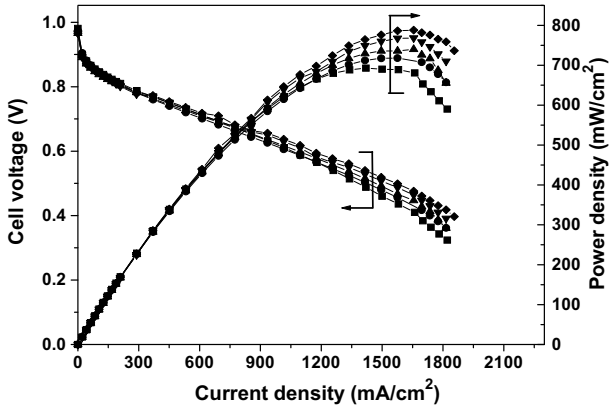

Fig. 7 – Galvanostatic polarization data for H_2/O_2 PEFCs comprising MEAs with GDLs of varying carbons, (▲) Vulcan XC-72R, (■) as prepared MC and MC treated with (●) 1, (♦) 2 and (▼) 3 M HNO_3.

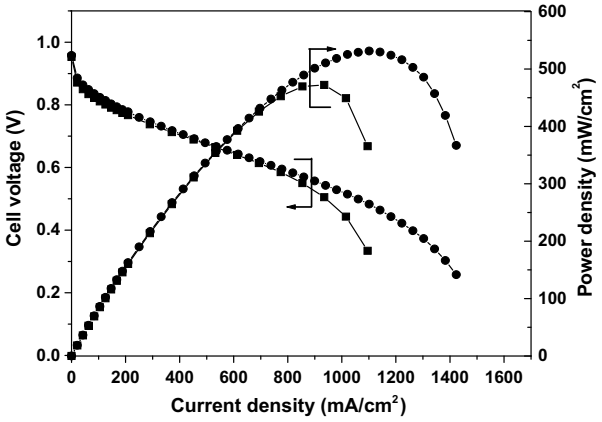

Fig. 8 – Galvanostatic polarization data for H_2/air PEFCs comprising MEAs with GDLs of different carbon, (■) Vulcan XC-72R and (●) MC treated with 2 M HNO_3.

The nitric acid treatment of the MCs besides creating the surface oxygen-groups also has an influence on both their pore diameter and pore volume. Fig. 2b suggests the pore volume to increase almost twice for small pores (3.8 nm) for the treated MC. By contrast, the pore volume for large pores is not affected and instead the pore diameter reduces from 7.6 to 6.4 nm. Due to the presence of different pore sizes in the GDL, the product water generated during the fuel cell operation can be easily removed through the smaller pores due to capillary action. The larger pores help permeation of reactant gases to the active catalyst site. As a result, the mass-transfer region in the PEFC is observed at a relatively higher load current-density and particularly so when air is used on oxidant side of the fuel cell. The MC treated with 3 M HNO_3 delivers a little lower power density possibly due to the partial damage of the mesoporous nature [28]. It is believed that the MEAs constituting MC treated with 2 M HNO_3 carbon create maximum oxygen surface groups without much destruction of structural features of the MC and hence this condition is taken as the optimal level of functionalization for fuel cell performance in this study.

The influence of the MC treated with 2 M HNO_3 is also analyzed for H_2/air PEFCs performance at 70 °C and atmospheric pressure and the results are compared with commercially available Vulcan XC-72R as shown in Fig. 8.

It is interesting to note that a peak power density of 0.53 W/cm^2 at a load current- density of 1.1 A/cm^2 is achieved for the PEFC electrode with MC treated with 2 M HNO_3 as compared to the peak power density of only 0.47 W/cm^2 at a load current-density of 0.9 A/cm^2 for the PEFC electrode with Vulcan XC-72R. Increase in power density of PEFC of H_2/air system with MC treated with 2 M HNO_3 near high current-density region is a clear manifestation of improved reactant-gas distribution as observed from the gas-permeability data presented in Fig. 6 and the subsequent product water removal.

4. Conclusions

A MC of high specific surface area and pore size is successfully synthesized by a soft-template route and utilized for

the first time, to our knowledge, as GDL in electrodes for PEFCs. The MC treated with 2 M HNO_3 ameliorates the fuel cell performance with little effect on its surface area and pore size. Due to the presence of different pore sizes in the GDL, both the product water removal and the gas permeability to the active catalyst sites are ameliorated.

Acknowledgments

Financial support from CSIR, New Delhi as a Supra Institutional Project is gratefully acknowledged. We thank Professor T.N. Guru Row, Ms. A. Jalajakshi and Dr. A.S. Prakash for their invaluable help.

REFERENCES

[1] Sinha PK, Mukherjee PP, Wang CY. Impact of GDL structure and wettability on water management in polymer electrolyte fuel cells. J Mater Chem 2007;17:3089–103.
[2] Williams MV, Begg E, Bonville L, Kunz HR, Fenton JM. Characterization of gas diffusion layers for PEMFC. J Electrochem Soc 2004;151:A1173–1180.
[3] Jordan LR, Shukla AK, Behrsing T, Avery NR, Muddle BC, Forsyth M. Diffusion layer parameters influencing optimal fuel cell performance. J Power Sources 2000;86:250–4.
[4] Neergat M, Shukla AK. Effect of diffusion layer morphology on the performance of solid polymer direct methanol fuel cells. J Power Sources 2002;104:289–94.
[5] Li W, Liang C, Zhou W, Qiu J, Zhou Z, Sun G, et al. Preparation and characterization of multiwalled carbon nanotube-supported platinum for cathode catalysts of direct methanol fuel cells. J Phys Chem B 2003;107:6292–9.
[6] Bessel CA, Laubernds K, Rodriguez NM, Baker RTK. Graphite nanofibers as an electrode for fuel cell applications. J Phys Chem B 2001;105:1115–58.
[7] Wang H, Chowalla M, Sano N, Jia S, Amaratunga GAJ. Large-scale synthesis of single-walled carbon nanohorns by submerged arc. Nanotechnology 2004;15:546–50.
[8] Wang JN, Zhao YZ, Niu JJ. Preparation of graphitic carbon with high surface area and its application as an electrode material for fuel cells. J Mater Chem 2007;17:2251–6.
[9] Tamai H, Sumi T, Yasuda H. Preparation and characteristics of fine hollow carbon particles. J Colloid Interf Sci 1996;177:325–8.
[10] Kannan AM, Veedu VP, Munukutla L, Ghasemi-Nejhad MN. Nanostructured gas diffusion and catalyst layers for proton exchange membrane fuel cells. Electrochem Solid State Lett 2007;10:B47–50.
[11] Su FB, Zeng JH, Bao XY, Yu YS, Lee JY, Zhao XS. Preparation and characterization of highly ordered graphitic mesoporous carbon as a Pt catalyst support for direct methanol fuel cells. Chem Mater 2005;17:3960–7.
[12] Joo SH, Pak C, You DJ, Lee SA, Lee HI, Kim JM, et al. Ordered mesoporous carbons (OMC) as supports of electrocatalysts for direct methanol fuel cells (DMFC): effect of carbon precursors of OMC on DMFC performance. Electrochim Acta 2006;52:1618–26.
[13] Wikander K, Ekstrom H, Palmqvist AEC, Lundblad A, Holmberg K, Lindbergh G. Alternative catalysts and carbon support material for PEMFC. Fuel Cells 2006;6:21–5.
[14] Ryoo R, Joo SH, Kruk M, Jaroniec M. Ordered mesoporous carbons. Adv Mater 2001;13:677–81.
[15] Lee J, Kim J, Hyeon T. Recent progress in the synthesis of porous carbon materials. Adv Mater 2006;18:2073–94.
[16] Joo SH, Choi SJ, Oh I, Kwak J, Liu Z, Terasaki O, et al. Ordered nanoporous arrays of carbon supporting high dispersions of platinum nanoparticles. Nature 2001;412:169–72.
[17] Wan Y, Yang HF, Zhao DY. Host-guest chemistry in the synthesis of ordered nonsiliceous mesoporous materials. Acc Chem Res 2006;39:423–32.
[18] Liang CD, Hong KL, Guiochon GA, Mays JW, Dai S. Synthesis of a large-scale highly ordered porous carbon film by self-assembly of block copolymers. Angew Chem Int Ed 2004;43:5785–9.
[19] Tanaka S, Nishiyama N, Egashira Y, Ueyama K. Synthesis of ordered mesoporous carbons with channel structure from an organic–organic nanocomposite. Chem Commun 2005;16:2125–7.
[20] Liang CD, Dai S. Synthesis of mesoporous carbon materials via enhanced hydrogen-bonding interaction. J Am Chem Soc 2005;128:5316–7.
[21] Wang X, Liang C, Dai S. Facile synthesis of ordered mesoporous carbons with high thermal stability by self-assembly of resorcinol–formaldehyde and block copolymers under highly acidic conditions. Langmuir 2008;24:7500–5.
[22] Zhang FQ, Meng Y, Gu D, Yan Y, Yu CZ, Tu B, et al. A facile aqueous route to synthesize highly ordered mesoporous polymers and carbon frameworks with Ia-3d bicontinuous cubic structure. J Am Chem Soc 2005;127:13508–9.
[23] Meng Y, Gu D, Zhang FQ, Shi YF, Yang HF, Li Z, et al. Ordered mesoporous polymers and homologous carbon frameworks: amphiphilic surfactant templating and direct transformation. Angew Chem Int Ed 2005;44:7053–9.
[24] Hampsey JE, Hu Q, Rice L, Pang J, Wu Z, Lu Y. A general approach towards hierarchical porous carbon particles. Chem Commun 2005:3606–8.
[25] Lakshmi N, Rajalakshmi N, Dhathathreyan KS. Functionalization of various carbons for proton exchange membrane fuel cell electrodes: analysis and characterization. J Phys D: Appl Phys 2006;39:2785–90.
[26] Zhao XS, Su F, Yan Q, Guo W, Bao XY, Lv L, et al. Templating methods for preparation of porous structures. J Mater Chem 2006;16:637–48.
[27] Raghuveer V, Manthiram A. Mesoporous carbons with controlled porosity as an electrocatalytic support for methanol oxidation. J Electrochem Soc 2005;152:A1504–1510.
[28] Bazuła PA, Lu AH, Nitz JJ, Schuth F. Surface and pore structure modification of ordered mesoporous carbons via a chemical oxidation approach. Micropor Mesopor Mater 2008;108:266–75.